#### Research Article

Yongcheng Ji\*, Zheng Li<sup>#</sup>, Wenyuan Xu, and Wei Li\*

# Mechanical damage mechanism investigation on CFRP strengthened recycled red brick concrete

https://doi.org/10.1515/rams-2023-0178 received May 22, 2023; accepted January 12, 2024

**Abstract:** Three reinforcement ratios (0, 50, and 100%) of carbon fiber reinforced plastics (CFRP) were selected to improve the mechanical properties of recycled brick concrete in this study. Utilizing axial compression test, X-ray diffractometer analysis, the evolution of parameters such as compressive strength, peak stress, and elastic modulus of reclaimed concrete were analyzed. The reclaimed brick concrete' stress distribution and damage mechanism were revealed. The aggregate internal failure and CFRP reinforcement effect mechanism are discussed. The finite element model of red brick concrete reinforced by CFRP under uniaxial compression is established. The constitutive model for CFRP-reinforced recycled brick concrete is proposed.

**Keywords:** recycled red brick concrete, CFRP reinforcement, mechanical property, finite element model, constitutive model

# 1 Introduction

The rapid development of the construction industry has led to a need for more natural resources and pollution of the environment in the past decades. It is estimated to consume nearly 17.5 billion tons of concrete [1,2]. Construction and demolition waste from demolished buildings,

# These authors contributed equally to this work and should be considered first co-authors.

**Zheng Li, Wenyuan Xu:** School of Civil Engineering and Transportation, Northeast Forestry University, Harbin 150040, China

including concrete, red brick, asphalt, and wood, is often sent to landfills, which hurts the environment [3]. Therefore, the recycling of construction waste has become an increasingly important issue. To conform to the concept of green development, the construction industry has begun to use recycled concrete. Recycled concrete uses the demolition waste after breaking as recycled aggregate, partially or entirely replacing the natural aggregate when new concrete is poured [4,5]. It is considered one of the most economical and environmentally friendly ways to recycle construction waste by using broken demolition waste as recycled aggregate. Using recycled aggregate instead of natural aggregate can effectively solve the problem of resource shortage and environmental pollution [6,7].

Recycled aggregate has the advantages of environmental protection and resource-saving. However, the recycled aggregate's poor mechanical properties will adversely impact recycled concrete's mechanical properties and durability, resulting in a limited application range. Yang et al. [8] revealed that the compressive strength of reclaimed concrete with 50% recycled aggregate content was reduced by 20%. Chen et al. [9] introduced red brick as the variable of recycled concrete. They constructed a new stress-strain constitutive relation expression consistent with the test results when the substitution rate of coarse aggregate was less than 50%. Xin et al. [10] studied the influence of waste brick aggregate on the compressive and shrinkage performance of recycled concrete by taking the volume substitution rate of waste to coarse aggregate as the change factor. The results show that when the equal volume replacement rate of waste brick is 25%, the water absorption treatment can improve the shrinkage deformation resistance of recycled concrete and has no noticeable effect on reducing the compressive strength of recycled concrete. To improve the performance of recycled concrete, many researchers use microscopic tests to explore the failure mechanism of the recycled aggregate itself. Xiao et al. [11] found that the reclaimed aggregate concrete has two interfacial transition zones (ITZs), one between the reclaimed aggregate concrete and the new mortar matrix and the other between the reclaimed aggregate concrete's original aggregate and the old mortar. The old mortar of reclaimed aggregate concrete comprises many pores and

<sup>\*</sup> Corresponding author: Yongcheng Ji, School of Civil Engineering and Transportation, Northeast Forestry University, Harbin 150040, China, e-mail: yongchengji@outlook.com

<sup>\*</sup> Corresponding author: Wei Li, School of Civil Engineering and Transportation, Northeast Forestry University, Harbin 150040, China, e-mail: alice12383@126.com

cracks, forming the weak link of reclaimed aggregate concrete. Ma *et al.* [12] found that SEM images showed that increasing the amount of regenerated aggregate within a specific range could improve the integrity of the specimen itself so that aggregate and other components could generate more aggregates. Yang *et al.* [13] investigated the shear properties of concrete with different recycled aggregate contents at different temperatures and found that after exposure to high temperatures, the recycled red brick aggregate content had little effect on the shear strength. Also, Yang *et al.* [14] found that limestone powder accelerated the hydration of cement by studying the effect of limestone powder on the microstructure of concrete.

Reinforced concrete structure often results in premature failure and deformation due to the failure of concrete, which leads to more significant economic losses. The strength of recycled concrete itself is low, so we should fully consider the consequences caused by the failure in advance. Because of the poor performance of recycled concrete, the use of carbon fiber cloth to strengthen recycled concrete specimens has been increasing in recent years. The technology of carbon fiber reinforced plastics (CFRP) can overcome the defects of sudden, brittle failure and delamination, which are common in traditional composites. The composite material made with epoxy coating CFRP has better delamination resistance, toughness, bearing capacity, and fatigue resistance, which can avoid these shortcomings [15]. Carbon fiber has the advantages of high strength, high elastic modulus, lightweight, convenient construction, energy saving, and environmental protection, so it is widely used in the transportation and construction industries. Because of the above advantages of CFRP, it has been widely used in concrete reinforcement technology. CFRP material can significantly boost the strength and deformation capacity of concrete, and CFRP reinforcement technology can improve the mechanical properties of the original structure. Studies have shown that [16] the ultimate bearing capacity of concrete will be further improved when large deformation FRP is used. Therefore, due to CFRP's larger elastic modulus and tensile strength, the mechanical properties of reclaimed concrete reinforced by CFRP are better than those reinforced by other fiber cloth.

Rajai *et al.* [17] established a three-dimensional finite element model to study the mechanical properties of circular concrete columns under different configuration constraints. The CFRP reinforcement can significantly improve axial strength and slightly increase the ultimate displacement. Chen *et al.* [18] studied the mechanical properties of aluminum alloy concrete columns strengthened by CFRP by combining tests and simulations. The ultimate bearing capacity and energy absorption capacity of specimens increased by 60.0 and 37.3%, respectively, which also

effectively inhibited the development of damage to specimens. Liu et al. [19] studied the changes in mechanical properties of lightweight aggregate concrete strengthened by CFRP, found that the strength of specimens strengthened by CFRP could be increased to 1.5 times at the highest level, and established peak stress and related strain models. Although CFRP can effectively improve the strength of concrete, the mechanical properties of the CFRP reinforcement system will be significantly reduced after the failure of the CFRP bond with concrete. Some scholars have proposed many methods combining experiment and theory given this situation. Ramirez et al. [20] studied the mechanical properties of specimens reinforced with external adhesive fiber cloth under different environments. The results showed that the aging and corrosion of FRP adhesive force would reduce the mechanical properties of specimens. Concrete layer stripping, interfacial debonding between concrete and binder, and bond layer shear failure are common interfacial failure forms [21]. As concrete is a heterogeneous material, many micro-cracks and pores will inevitably be formed when manually mixing, setting, and polishing the surface. Adhesive bond failure mainly occurs in the concrete layer near the adhesive-concrete interface. The bond strength depends on the shear strength of the concrete surface. The presence of these cracks and pores will cause the shear strength to decrease, so the binder may not be fully utilized. Several scholars have conducted much research on the bond strength of FRP systems. Some research focuses specifically on the axial stiffness, width, length, and type of FRP strips, as well as the effect of concrete strength on bond strength and other parameters. The bonding behavior of the interface between CFRP and concrete is a critical factor for the debonding failure of recycled concrete reinforced structures [22]. The bond strength mainly depends on the concrete's strength and the CFRP material's characteristics, including CFRP's thickness, width, elastic modulus, and interfacial fracture energy [23]. Interfacial fracture energy (GF) is the area under the bond–slip curve and is one of the most critical parameters affecting bond strength. Generally, interfacial fracture energy depends on concrete strength, the width ratio of CFRP sheet to concrete specimen, the length-diameter ratio of interfacial failure surface, concrete surface roughness, aggregate type, water-cement ratio, and bonding layer thickness [24].

In summary, the research on the mechanical numerical analysis model of recycled aggregate concrete and the mechanical behavior under the influence of parameters such as recycled aggregate content has been completed. The research on the bonding mechanism between concrete and CFRP is also relatively complete. However, there needs to be more research on concrete microstructure due to the

need for correlation mechanisms before and after fiber reinforcement. In addition, different reinforcement methods of recycled aggregate and fiber cloth will lead to different bonding modes of CFRP reinforcement system, affecting the constitutive relationship and resulting in unclear research on the mechanical properties of fiber-reinforced recycled concrete. Most research has focused on incorporating different types of fibers in the design of recycled concrete mixes to improve their mechanical properties, which can only be applied to new structures. For the carbon fiber-reinforced recycled concrete structure, the influence of fiber interface strengthening on its overall mechanical properties is relatively tiny. The change law of this composite structure's stress-strain relationship under load needs further study.

To understand the mechanical properties of carbon fiber-reinforced recycled concrete, the mechanical properties of each component material and the whole reinforced structure need further study. Moreover, the influence of recycled aggregate on the concrete structure itself accurately reveals the damage evolution law of the interface structure and builds a refined numerical model. Three replacement rates of 0, 50, and 100% recycled aggregate were made in this study. Three reinforcement methods of unreinforced, semi-reinforced, and fully reinforced specimens were tested. The specimen's axial compressive strength, elastic modulus, and stress-strain trend were measured. Furthermore, specimens with different red brick content were selected for microscopic observation of the fracture surface, and the failure mechanism was analyzed by observing inside specimens with SEM. The random recycled aggregate and CFRP reinforcement models were established using finite element simulation software for numerical simulation and analysis. The test results confirmed the validity of the simulation analysis and established the constitutive model of regenerated concrete reinforced red brick with CFRP. It has important guiding significance for this new reinforced structure's mechanical property design and engineering application.

# 2 Materials and tests

### 2.1 Test material and test mix ratio

#### 2.1.1 Test materials

Concrete with a designed strength grade of C30 is used in the test, and its composition materials include water, cement, sand, and gravel, as shown in Figure 1. The specific mix ratio is shown in Table 1. Cement used by Jilin Yatai Cement Co., LTD. Swan brand P.O. 42.5 ordinary Portland cement. The fine aggregate was medium sand with a modulus coefficient of 2.4. The coarse aggregate is macadam, in which the particle size of 5~10 mm accounts for 30% and 10-20 mm for 70%. Table 2 shows the specific particle gradation, and it meets the continuous grading requirements stipulated in Pebble and crushed stone for construction (GB/T14685-2011) [25].

The experimental test adopts the unidirectional carbon fiber cloth and the matching resin adhesive of the Ruishi brand, wherein the resin adhesive is divided into A and B, two components. Group A was divided into epoxy resin, translucent opalescent white, and group B was divided into curing agent, dark red, the thickness of carbon fiber cloth is 0.167 mm. The performance indexes of the two materials are shown in Tables 3 and 4, which meet the requirements of the safety appraisal of engineering structural strengthening materials (GB50728-2011) [26].

Table 1: Concrete mix ratio

Material	Water	Cement	Medium sand	Crushed stone
Content (kg·m <sup>-3</sup> )	209	387	635	1,169



Figure 1: Composition materials: (a) cement; (b) medium sand; and (c) red brick aggregate.

#### 2.1.2 Test mix ratio

To study the effects of different regenerated aggregate replacement rates on the mechanical properties of red brick specimens, and the effect on concrete is small when the regenerated aggregate replacement rate is less than 25%, three kinds of regenerated aggregate replacement rates of red brick are designed, including 0, 50, and 100%. The replacement rate of a recycled aggregate of red brick is calculated by volume fraction due to the light aggregate quality. The density of natural aggregate is 2,794 kg·m<sup>-3</sup>, and the density of recycled aggregate is 2,130 kg·m<sup>-3</sup>. The specific coordination in the test is shown in Table 5.

# 2.2 Specimen preparation and number

To prevent stress concentration when wrapped with a carbon fiber cloth, cylindrical specimens were used for the axial compression test in this test. Moreover, according

Table 2: Aggregate composition of coarse aggregate

Square hole screen size (mm)	GB/T 14685-2011 provides for the cumulative sieve residual (%)	Test cumulative sieve (%)
2.36-4.75	95–100	100
4.75-9.50	90–100	97
9.50-16.0	40-80	67
16.0-19.0	_	34
19.0-26.5	0–10	2

to the research of Deng *et al.* [27], if the diameter of the cylindrical fiber-reinforced concrete specimen is larger than 50 mm, the influence of the specimen size is extremely limited, and the specimen size can be normally restrained and tested. The size of the specimens was 100 mm × 200 mm (bottom diameter × height). To study the influence of different CFRP reinforcement ratios on recycled red brick concrete, three kinds of axial compression specimens with 0, 50, and 100% reinforcement ratios were designed, which were respectively recorded as unreinforced axial compression specimens, and fully reinforced axial compression specimens, and fully reinforced axial compression specimens. After considering the reinforcement ratio and the replacement rate of red brick, there are nine groups of four specimens in each group.

The specimens of unreinforced concrete axial compression are not strengthened. Instead, the semi-reinforced concrete specimens are reinforced by five CFRP strips with a width of 20 mm, and the apparent distance between the CFRP strips is 25 mm. A CFRP strip with a width of 200 mm is used to paste the fully reinforced concrete axial compression specimen. In addition, the upper and lower bottom surfaces of fully reinforced and semi-reinforced concrete specimens must be coated with epoxy resin. CFRP has two failure modes: fracture of the fibers themselves or failure of the interfacial bond at the interface of the CFRP strips. The first failure mode can give full play to the mechanical properties of CFRP. To ensure the reinforcement effect and give full play to the mechanical properties of CFRP, the interfacial bonding at the interface must be enforced, and the two edges of the CFRP strips must have sufficient displacement length for lap splicing. The lap length is 1/4 of the circular section circumference of the specimen to ensure that CFRP interface debonding can

Table 3: Properties of epoxy resin adhesive

Inspection item	GB 50728-2011 qualified index	Merchant measurement index
Tensile strength (MPa) Modulus of elasticity under tension (MPa) Elongation (%)	≥38 ≥2.4 × 10 <sup>3</sup> ≥1.5	55.1 2.71 × 10 <sup>3</sup> 2.41

Table 4: Properties of carbon fiber cloth

Inspection item	GB 50728-2011 qualified index	Merchant measurement index
Tensile strength (MPa)	≥3,400	3,520
Modulus of elasticity under tension (MPa)	≥2.3 × 10 <sup>5</sup>	2.68 × 10 <sup>5</sup>
Elongation (%)	≥1.6	1.77

be prevented. Concrete specimen reinforcement steps are as follows:

- 1) The reinforcement part of the concrete axial compression specimen is roughened.
- 2) Both pre-cut carbon fiber cloth sides are coated with epoxy resin glue. Then the carbon fiber cloth soaked by resin glue is pasted on the reinforcement part of the axial compression specimen. Finally, the resin glue is applied on the bottom surface of the upper and lower sides of the axial compression specimen.
- The axial compression specimen was placed at room temperature for 7 days until the resin adhesive was completely cured.

#### 2.3 Test method

#### 2.3.1 Mechanical properties test (compressive test)

To discuss the constitutive relationship of specimens of CFRP regenerated concrete, axial compression tests were conducted on specimens following the provisions of the Standard for test methods of concrete physical and mechanical properties of Concrete (GBT50081-2019) [28]. The axial compression test equipment includes the mechanical control and data acquisition system. The former loads the specimen by controlling the YAM-5000F electro-hydraulic servo hydraulic pressure testing machine. The latter collects data through strain gauges and strain tanks, as shown in Figure 2. The strain gauge is longitudinally attached to 1/2 height of the axial compression specimen side surface along the height of the concrete. For unreinforced specimens, it is directly attached to the concrete side surface, and the reinforced specimens are attached to the outer surface of the fiber cloth until the concrete is damaged, and the deformation of the two specimens is consistent, which will not cause error in the result, and the change of concrete longitudinal strain is measured.

#### 2.3.2 Microstructure observation

The GAOSUO digital microscope observes the side and internal failure surfaces. The observation multiple is 100

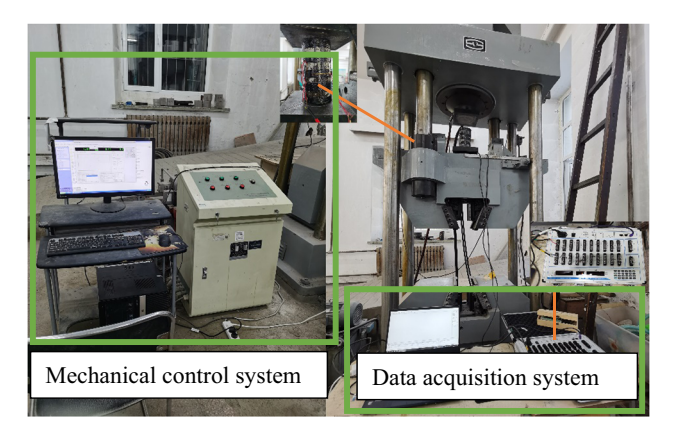
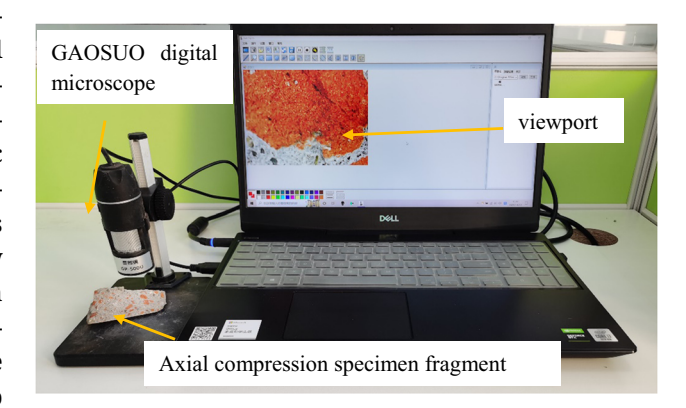


Figure 2: Mechanical test equipment.



**Figure 3:** Microobservation equipment for failure section of axial compression specimen.

Table 5: Mix ratio of concrete specimens (kg·m<sup>-3</sup>)

Specimen set	Water	Cement	Medium sand	Natural coarse aggregate	Recycled coarse aggregate	Carbon fiber reinforcement ratio	Red brick replacement rate
CF0-RA0	209	387	635	1,169	0	0	0
CF50-RA0	209	387	635	1,169	0	50%	0
CF100-RA0	209	387	635	1,169	0	100%	0
CF0-RA50	209	387	635	585	446	0	50%
CF50-RA50	209	387	635	585	446	50%	50%
CF100-RA50	209	387	635	585	446	100%	50%
CF0-RA100	209	387	635	0	891	0	100%
CF50-RA100	209	387	635	0	891	50%	100%
CF100-RA100	209	387	635	0	891	100%	100%

6 — Yongcheng Ji et al. DE GRUYTER

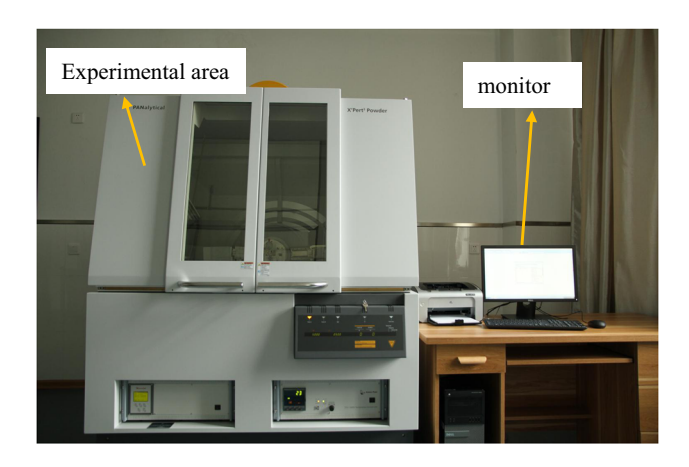


Figure 4: XRD diffraction instrument.

times, as shown in Figure 3. The failure mechanism of the axial compression specimen was also studied. The debris of the specimen damaged by the axial compression test was selected, washed, and dried. The failure surface of the axial compression specimen was observed.

## 2.3.3 X-ray diffractometer (XRD) analysis

The XRD carried out the phase analysis. First, take part of the test blocks, grind them into a fine powder with a uniform particle size of about 5–10  $\mu$ m and more than 5 mg, then put them into a vacuum drying oven at 50°C for 24 h for testing, as shown in Figure 4.

# 3 Results and discussion

# 3.1 Compressive strength

The concrete damage patterns for axial compression of CFRP recycled concrete with different reinforcement ratios are shown in Figure 5. It can be observed that with the increase of reinforcement ratio, the reclaimed concrete specimen after failure becomes integrity. No apparent phenomenon occurred in the initial stage of axial compression test loading. With the axial pressure test, tiny cracks appeared on the concrete surface. With the load increase, the number and length of small cracks gradually increase. At the same time, small cracks extend to several intermittent longitudinal cracks and continue to overlap each other. Figure 5(a) shows the axial compression specimen of unreinforced recycled concrete. On the other hand, there is no evident phenomenon in the initial loading stage

for the semi-reinforced recycled concrete axial compression specimens. With the increase in load, small cracks in the unprotected part of the sample develop slowly. It is because CFRP has a radial binding force for reclaimed concrete to prevent the creation and development of cracks. Once the load is 70% of the final load capacity of the concrete, it will cause continuous, slight cracks and partial cracks in the epoxy resin bonding. The test concrete makes a loud "click" sound as the load achieves the limited load capacity of the test slab. The three CFRP strips in the center immediately fracture, accompanied by cracks in the concrete fragments and epoxy rubber chips. The specimens exhibit apparent brittle damage, and the damage morphology of the semi-reinforced axial compression specimens is shown in Figure 5(b). The damage pattern of fully reinforced reclaimed concrete specimens is similar to that of semi-reinforced concrete specimens, and there is no apparent phenomenon at the initial loading stage. As the load achieves 80% of the ultimate bearing capacity of the specimens, there is a continuous and slight "click" sound from the specimens, and cracks appear in some of the epoxy resin adhesives. The test specimen emits a loud "click" sound when the load reaches the ultimate bearing capacity of the specimen. The CFRP strips in the middle and top regions of the concrete fracture instantly, followed by the bursting of concrete and epoxy glue fragments. Specimens indicate apparent brittle damage, and the damage morphology of the fully reinforced axial compression specimens is shown in Figure 5(c).

Figure 6 shows that different replacement rates of red brick affect the compressive strength of concrete. The general trend is that the strength of recycled concrete samples gradually decreases with the increase of red brick content. For example, compared with the concrete without red brick aggregate, the strength of the specimens with 50 and 100% mixture decreased by 14 and 29%, respectively. It is mainly due to the immense void of the red brick aggregate itself, the high water absorption rate, and the low strength of recycled aggregate. On the other hand, the overall compressive strength of CFRP-reinforced specimens is higher than that of unreinforced specimens. Taking 50% red brick content as an example, compared with unreinforced specimens, the strength of specimens increased by 27 and 44%, respectively, after semi-reinforced and fully reinforced treatment, showing a nonlinear overall upward trend. In addition, even the specimens with a 100% red brick replacement rate can have the same compressive strength as plain concrete after complete reinforcement treatment. Therefore, the compressive strength of concrete can be significantly improved by wrapping carbon fiber cloth to offset the negative impact of



(a)



(b)



(c)

Figure 5: Failure morphology of specimens (from left to right are specimens with red brick aggregate replacement rate of 0, 50, and 100%): (a) failure state of unreinforced specimens, (b) failure state of semi-reinforced specimens, and (c) failure state of fully reinforced specimens.

the addition of recycled aggregate on the strength of concrete. Moreover, the effect of different replacement rates of regenerated red brick on strength under three reinforcement methods is fitted well ( $R^2 = 0.98$ ), as shown in Figure 7.

#### 3.2 Stress-strain curve

The stress-strain relationships for recycled aggregates with different substitution rates under axial compression tests are shown in Figure 8. The curves of specimens with

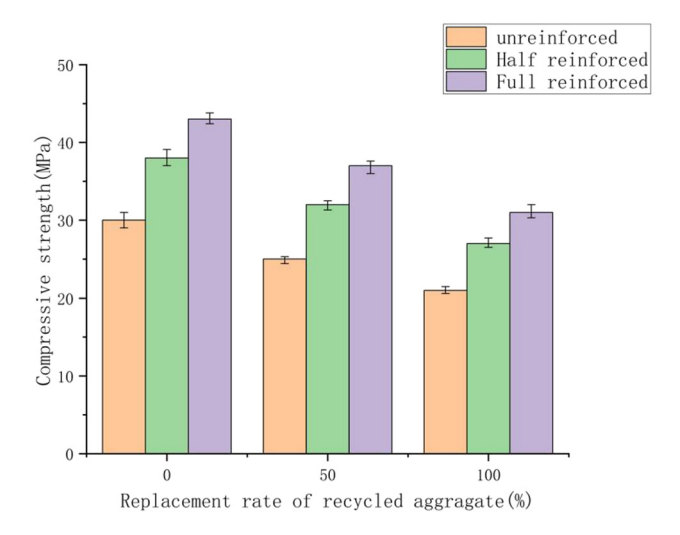


Figure 6: Compressive strength of recycled red brick with different.

different replacement rates have similar overall shapes and are composed of ascending and descending sections. However, there are significant differences in peak stress and peak strain. The maximum stress decreases with the increase of regenerated aggregate content, and the corresponding peak strain increases while the slope of the upward curve decreases gradually. The compressive strength of semi-reinforced specimens is 26% higher than that of unreinforced specimens, and that of fully reinforced specimens is 13% higher than that of semi-reinforced specimens. The results show that the slope of recycled concrete decreases with the increase in aggregate replacement rate. It is observed that with the increase in aggregate replacement rate, the decline curve becomes steeper, indicating that different samples have different ductility. The main reason is that the hardness of red brick aggregate is lower than that of natural aggregate. Compared to recycled concrete specimens with different reinforcement ratios, it can be found that the higher the reinforcement ratio, the more significant the difference in strength between ordinary concrete and red brick concrete. Therefore, CFRP reinforcement can improve concrete specimens' ultimate and peak strain. The higher the CFRP bonding area, the more pronounced the strain and compressive strength improvement effect.

Under axial compression load, the peak stress of concrete specimens corresponds to the strain, that is, the peak strain, which gradually increases with the increase of the red brick content. Figure 9 shows the maximum strain when the maximum load is generated on the stress–strain curve under different CFRP reinforcement conditions. The

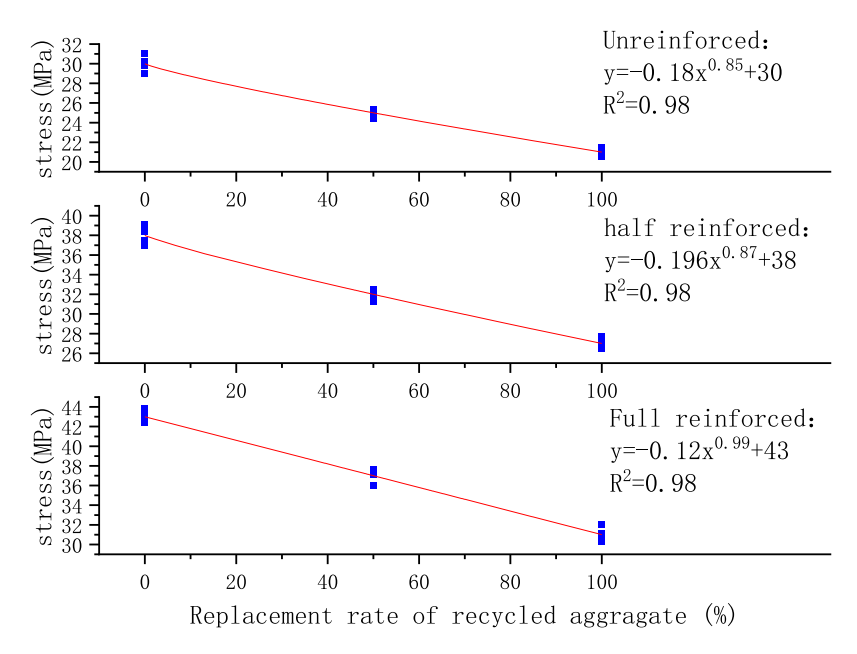


Figure 7: Strength fitting of recycled concrete under different replacement rates of recycled aggregate.

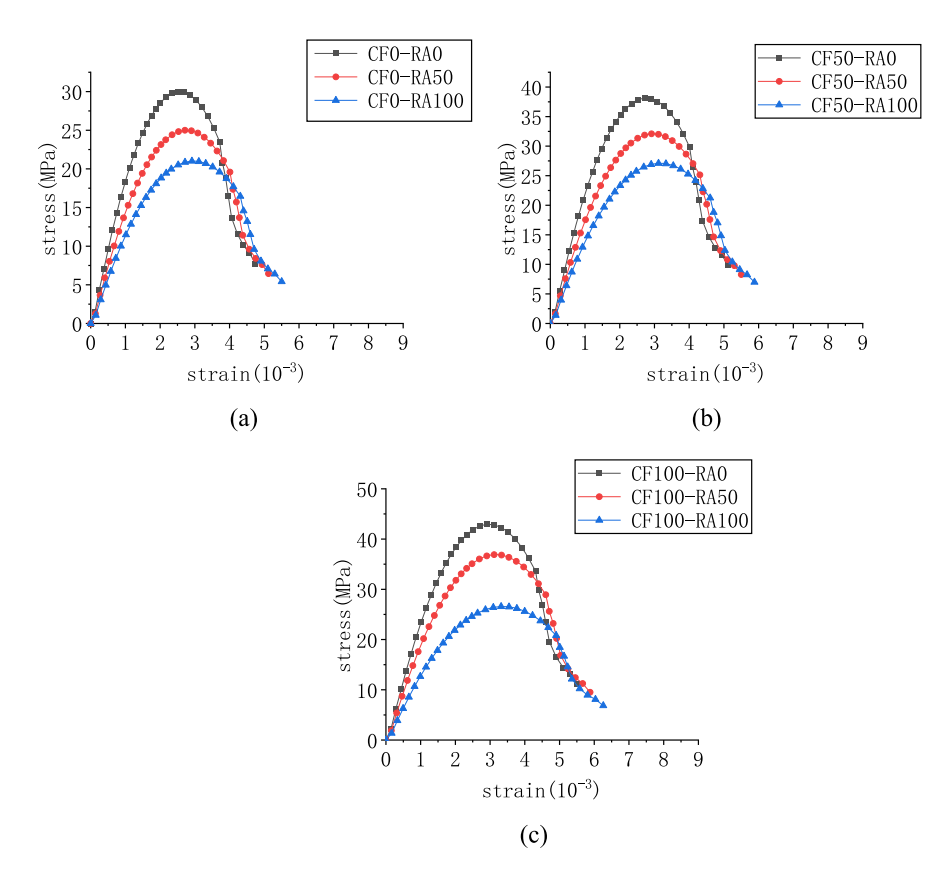


Figure 8: Stress-strain curve of CFRP reinforced red brick concrete: (a) unreinforced concrete; (b) half reinforced concrete; and (c) fully reinforced concrete;

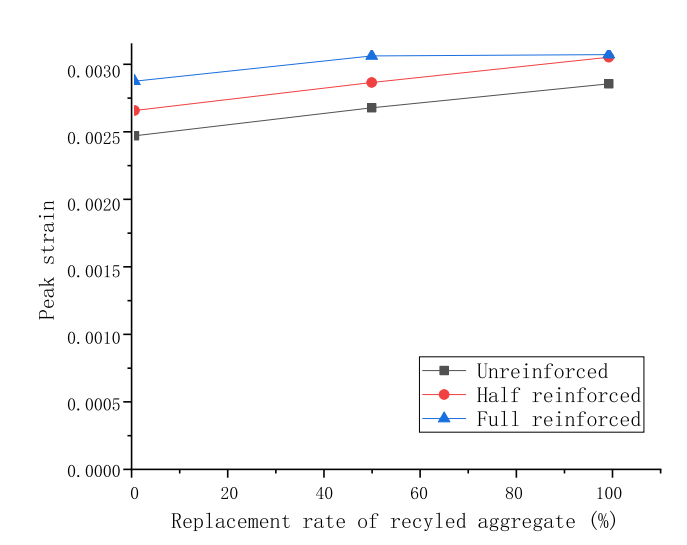


Figure 9: Peak strain of recycled concrete.

peak strain of reclaimed concrete is observed to be greater than that of plain concrete. The peak strain is positively correlated with the carbon fiber reinforcement rate and coarse aggregate replacement rate. With the increase in red brick aggregate replacement rate, the peak strain of concrete presents a linear increase trend. Compared with the concrete without the reinforcement of CFRP, when the aggregate replacement rate of red brick increases from 50 to 100%, the peak strain of concrete increases from 8.3 to 16%. Compared with the semi-reinforced recycled concrete specimens without red brick aggregate, the peak strain of the concrete specimens with 50 and 100% red brick aggregate replacement rates increases by 6.9 and 14.3%, respectively. Compared with those without red brick aggregate, the peak strain of the fully reinforced recycled concrete specimens with 50 and 100% red brick aggregate increased by 6.9 and 7.6%, respectively. When the aggregate replacement rate of red brick is 0%, the peak strain of semireinforced and fully-reinforced concrete specimens is increased by 8.4 and 15.5%, respectively, compared with that of unreinforced concrete specimens. When the aggregate replacement rate of red brick is 50%, the peak strain of semi-reinforced and fully reinforced concrete specimens increases by 7.8 and 14.8%, respectively, compared with unreinforced concrete specimens. When the aggregate replacement rate of red brick is 100%, the peak strain of semi-reinforced and fully reinforced concrete specimens increases by 6.5 and 6.8%, respectively, compared

with unreinforced concrete specimens. Although the peak strain of the specimen did not increase linearly, the overall trend was upward. For example, when the replacement rate of red brick aggregate reached 50%, the maximum peak strain of different reinforcement ratios showed an increasing trend. In addition, with the red brick replacement rate increase, the maximum peak strain of unreinforced, semi-reinforced, and fully reinforced specimens increases by 16, 14, and 7%, respectively, compared with those without red brick aggregate. Because the compactness of red brick aggregate is low, and the longitudinal strain is high during axial compression. Meanwhile, the CFRP reinforcement system can give full play to the hoop effect of concrete and further improve the peak strain.

The main reason for this phenomenon is: in the early stage of axial test loading, the weak part of the concrete specimen first appeared micro-cracks, the concrete itself lateral strain is low, and the CFRP lateral constraints are weak; with the increase of axial pressure the number of cracks inside the concrete increases, the core of the specimen of the cement and the recycled aggregate expansion, at this time, the edge of the concrete specimen is subjected to both the tensile force and the constraint force by CFRP; when the axial load reached the peak, the CFRP cloth breaks and interlayer damage occurs. When the axial load reaches the peak value, the CFRP fabric breaks and interlayer damage occurs. The strength of the recycled concrete decreases due to the incorporation of recycled aggregate, but the peak strain of the recycled concrete specimens is greater than that of the normal concrete due to the stronger bonding properties of the red brick aggregate and its softer texture compared to the natural aggregate. It agrees with the results obtained in the study by Yang et al. [29].

#### 3.3 Microstructure analysis

#### 3.3.1 Micro observation of failure surface

The damage of the regenerated red brick aggregate and carbon fiber cloth during the failure must be further studied. The failure mechanism of the CFRP-reinforced concrete can be studied by observing the specimen and its falling fragments after uniaxial compression with a digital microscope. The damaged section of concrete and the damaged place of carbon fiber cloth are observed under a GAOSUO digital microscope, and the magnification is 100 times. Through observation, it can be found that cracks

through the aggregate itself are generated during axial compression failure of concrete containing recycled red brick aggregate (Figure 10b), which leads to the destruction of the red brick aggregate itself. In addition, the sealing and cohesiveness of the mortar in the interface between the concrete and the transition region of the recycled aggregate became poor, and cracks through the transition region of the recycled aggregate and mortar were created (Figure 10c). Observing the recycled concrete strengthened with CFRP shows that the carbon fiber cloth used for reinforcement breaks along the length direction (Figure 10d). The CFRP reinforcement system gives full play to the mechanical properties of the carbon fiber material itself and effectively improves the axial compressive strength of the recycled concrete. On the other hand, it is observed that the epoxy resin adhesive bonded to CFRP and recycled concrete on the side is pulled off in the process of axial compression and that the epoxy resin coated on the upper and lower surfaces of the recycled concrete specimens also has cracks in the process of compression (Figure 10e), indicating that the epoxy resin has been bearing loads in the process of axial compression. It is only destroyed once the material's compressive strength is fully exerted. Therefore, the strength of reclaimed concrete strengthened by CFRP is improved compared with that of reclaimed concrete. However, different from the central damage zone in the failure of ordinary concrete, the failure of reclaimed concrete usually occurs at the reclaimed aggregate itself, then develops to the transition zone of the mortar interface.

#### 3.3.2 XRD analysis

Figure 11 shows 28 days XRD patterns of recycled red brick concrete and ordinary concrete samples. The chemical composition of cement is similar to that of red brick powder, except that the content of SiO is tiny, and the content of CaO is more. As depicted in Figure 11, the main mineral phases of the three XRD patterns are Ca (OH)<sub>2</sub>, CaCO<sub>3</sub>, C–S–H gel, SiO<sub>2</sub>, and Al<sub>2</sub>O<sub>3</sub>. The peak value of recycled red brick concrete is different from that of ordinary concrete because the main chemical composition of the red brick powder is SiO<sub>2</sub>, Fe<sub>2</sub>O<sub>3</sub>, and Al<sub>2</sub>O<sub>3</sub>, and it only contains a low amount of CaO. In addition, a large amount of Ca(OH)2 will be produced at the initial stage of cement hydration, making the slurry in an alkaline environment. The reason for CaCO<sub>3</sub> is that Ca(OH)<sub>2</sub> of cement hydration products reacts with CO2 in the air, which is the phenomenon of carbonization. Due to the more porous red brick, the carbonization of reclaimed red brick concrete is more

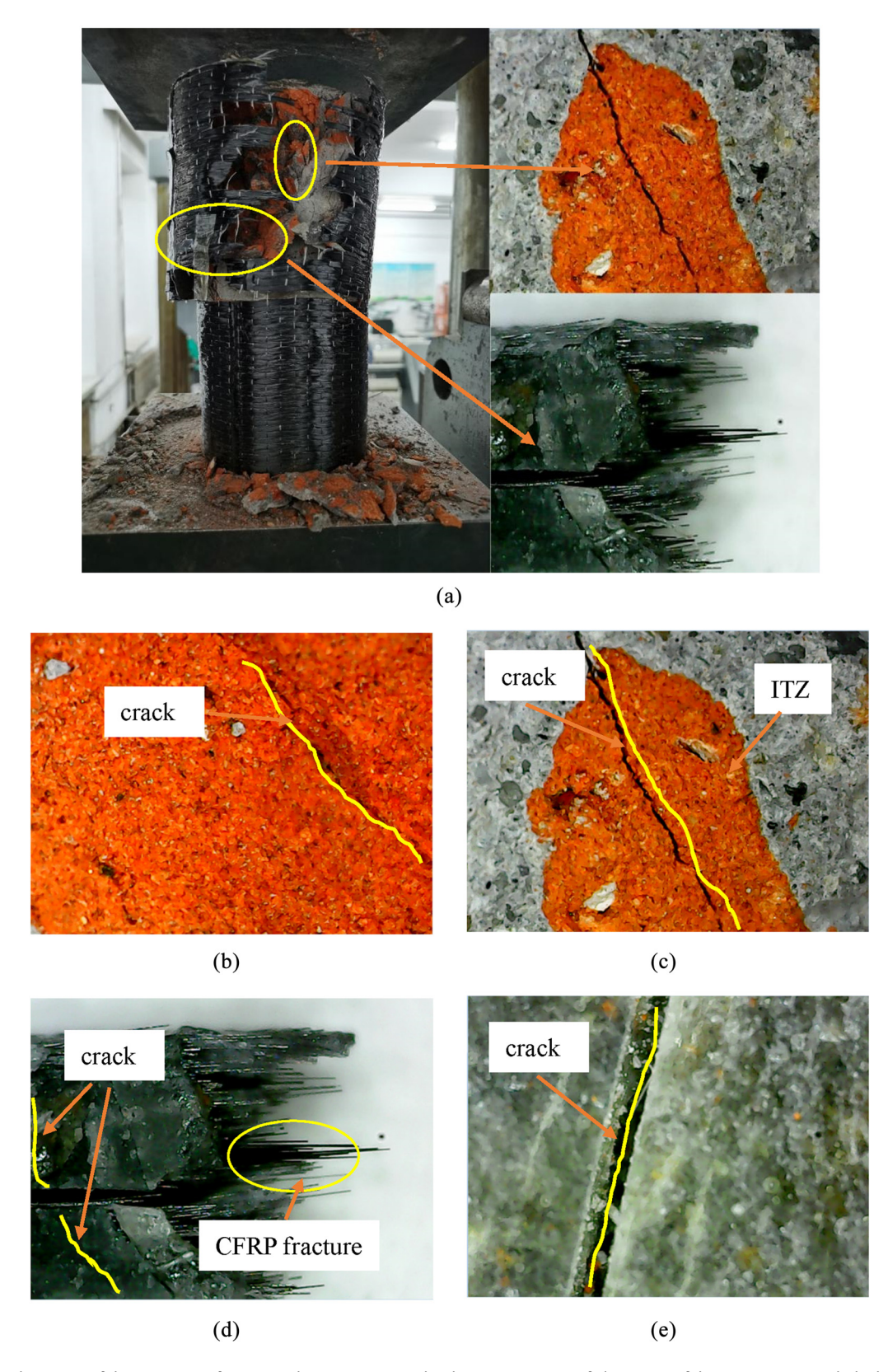


Figure 10: Failure state of the specimen after uniaxial compression under the microscope: (a) failure state of the specimen as a whole (b) failure state of the regenerated aggregate, (c) failure state of the regenerated aggregate and the transition zone, (d) failure state of CFRP and epoxy resin on the side surface, and (e) failure state of epoxy resin on the top surface.

12 — Yongcheng Ji et al. DE GRUYTER

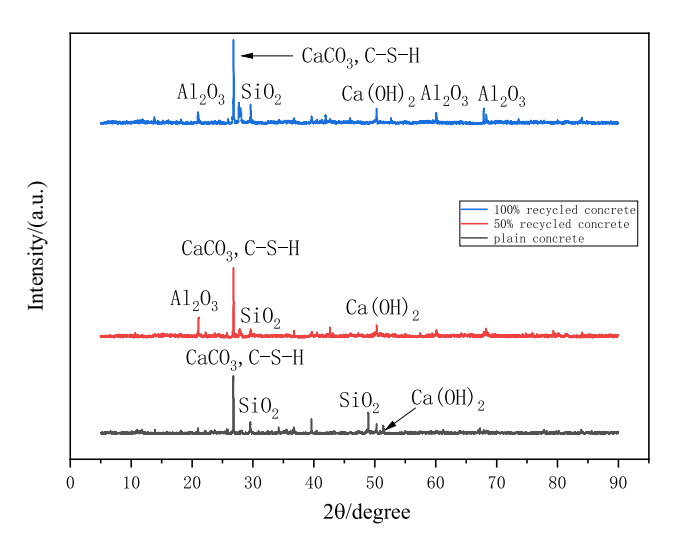


Figure 11: XRD analysis of 28-day samples.

likely than that of ordinary concrete, which harms the durability of reclaimed concrete products. The reason for the emergence of SiO2 is that many inactive SiO2 in the recycled concrete did not undergo a hydration reaction. As can be illustrated from Figure 11, the composition of reclaimed red brick concrete is mainly composed of Ca (OH)<sub>2</sub>, C-S-H gel generated by the hydration reaction of cement, CaCO<sub>3</sub>, and other hydration products produced by carbonization, and also contains some incomplete SiO<sub>2</sub>, which provides a source for the strength of reclaimed concrete. With the increase of red brick content, the peak value of CaCO<sub>3</sub> increases, indicating that the carbonization reaction is intensifying. It also leads to the deterioration of the mechanical properties of recycled concrete in another aspect. Compared with natural aggregate concrete, the distribution range of Al<sub>2</sub>O<sub>3</sub> in concrete mixed with red brick aggregate at different angles gradually increases with the increase of red brick content, but the strength decreases. Because of the increase of red brick content, the chance of red brick aggregate combining with cement mortar increases, but the combination of the red brick aggregate itself is not as good as the combination of natural aggregate, which leads to the decline of Al<sub>2</sub>O<sub>3</sub> strength to a certain extent. Compared with SiO<sub>2</sub>, which has little chance, Ca(OH)<sub>2</sub> changes significantly with the increase of red brick content. The distribution range of Ca(OH)<sub>2</sub> in the recycled concrete of red brick does not change significantly, but the strength increases to a certain extent. It is mainly because the red brick aggregate has a large void, which provides more opportunities for cement hydration reaction in the initial formation of the specimen. To provide specific strength support for the red brick aggregate recycled concrete.

# 3.4 Finite element model analysis

#### 3.4.1 Establishment of finite element model

The finite element model was established to verify the accuracy of the simulated values by comparing the test values, and an effective model was established to predict the strength and stress-strain curves of recycled concrete with the recycled aggregate replacement rate not involved in the test. CFRP-reinforced recycled concrete has two essential elements. Namely, recycled aggregate and CFRP reinforced system. However, the traditional ABAOUS model must analyze the relationship between recycled aggregate and cement base. The microscopic model of recycled aggregate and the axial compression model of CFRP-reinforced concrete are established further to study the effect of reclaimed aggregates on concrete. Recycled concrete mainly comprises aggregate, cement base, and ITZ, in which aggregate accounts for 60–70% of the total volume of concrete. To further study the failure mechanism of reclaimed concrete under axial compression and better observe the internal changes of concrete, a finite element model of randomly reclaimed aggregate was established by combining it with the microscopic test to reflect the microscopic structure of recycled concrete. Using ABAQUS to model and numerically analyze 2D reclaimed aggregate concrete. The aggregates were divided into three grades, and the transition zone at the interface was determined by numerical simulation to have a thickness of 0.5 mm. A two-dimensional finite element model was established to simulate the force analysis of the mid-point section of the diameter of the cylindrical specimen. The following three colors represent red brick aggregate, interface (ITZ), and base. The size of the model is 200 mm long and 100 mm wide. Constraints are set along the axial compression direction of the concrete model, and constraints are added in the horizontal direction of the midpoint at the bottom of the specimen to simulate the actual constraints of the specimen in the axial compression test. CPS3 units, with an average size of 1.0 mm, are used for meshing mortar matrix, aggregate, and ITZs. The three components, mortar matrix, aggregate, and ITZ, are grouped (Figure 12) (Table 6).

The integral axial compression model of CFRP regenerated concrete was established. In the axial compression test, the interior of the regenerated concrete for the CFRP reinforcement system is a whole, so C3D8R solid unit (8-node hexahedral linear reduction solid integral unit) was adopted to simulate the concrete material. CFRP is a material whose thickness is much smaller than that in other directions. Therefore, in finite element analysis, only the strength in the plane is considered. Therefore, the S4R shell

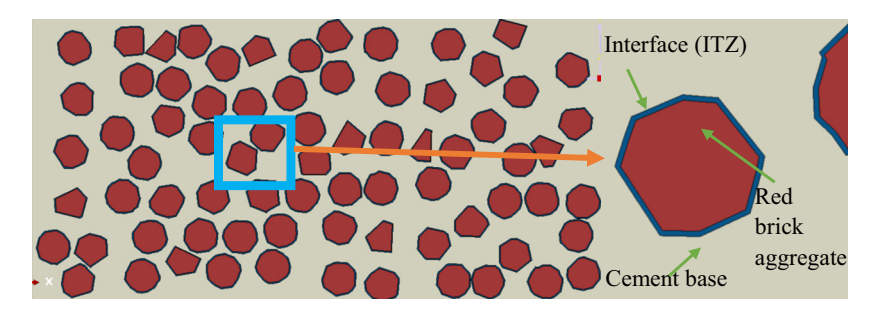


Figure 12: Establishment of random aggregate model.

Table 6: Material properties

Material properties	RBCA	NCA	Mortar matrix	ITZ	CFRP
Compressive strength (MPa)	18	144	28.96	16	_
Tensile strength (MPa)	5.1	9.6	1.988	1.6	3,400
Elastic modulus (MPa)	16,000	70,000	28,960	26,000	260,000
Poisson's ratio	0.20	0.16	0.2	0.2	0.2

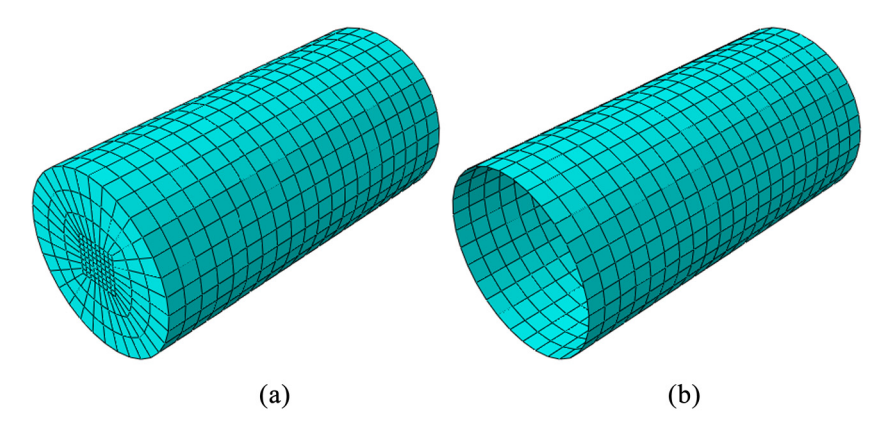


Figure 13: Building concrete and CFRP models: (a) concrete and (b) CFRP.

element (4-node quadrilateral linear reduction integral shell element) simulates CFRP material. Figure 13 shows the grid division of concrete and CFRP. The underlay block's 6 degrees of freedom (X, Y, Z, RXY, RYZ, RZX) were all fixed to simulate the finite element model loading scheme consistent with the test. To output load and displacement, the upper pad is coupled with the reference point RP1, and "hard contact" and no friction is used between the concrete and the indenter. Loading scheme: A concentrated linear force is applied to the reference point RP1, converted into a stress rate of 0.05 MPa·s<sup>-1</sup>. The test is stopped when CFRP reaches the ultimate strain, and the specimen is considered damaged.

#### 3.4.2 Analysis results of finite element model

The damage development of reclaimed aggregate concrete differs from that of ordinary concrete. The failure of recycled aggregate concrete first appears in the recycled aggregate itself, consistent with the microscopic observation. To obtain the damage of recycled concrete at different stress and strain stages, the ultimate stress and the ultimate strain corresponding to 60% of the post-peak ultimate stress are selected for analysis. It can be viewed from the finite element calculation results that the stress at the place where the load is applied is assumed as the only node, and the force-displacement curve is made. It can be observed

from XY data processing that frame 20 is the ultimate stress, and frame 476 is the 60% stress after the peak, that is, the ultimate strain. As discerned from the figure below, the edge of the red brick's regenerated aggregate and the interface's transition area marked in the figure of peak stress reaches the maximum current stress. The aggregate, as the center begins to show a V-shaped failure trend, the cement base begins to produce damage, and the crack gradually expands. It is evident that many red brick aggregates have been damaged, and the damage has penetrated through the red brick aggregate and the nearby cement base. The injured cracks progressively expand, and the specimen is damaged. The failure of the recycled concrete specimens first appeared in the interface transition region with poor mechanical behavior. The regenerated aggregate and mortar interface gradually appear damaged edge extension with the load increase. With the gradual development of damage at different locations, the regenerated aggregate breaks, leading to the specimen's failure (Figure 14).

Similarly, the simulation results of peak stress and ultimate strain at two moments of the CFRP strengthening system are also selected for analysis, corresponding to the 67th and 100th frames, respectively. It can be inferred from the observation of the occurrence time of peak stress that, due to the hoop effect of concrete, the stress on the core area of concrete in the same section is less than the surrounding stress. In the whole reinforced concrete, close to the pressure point of the side, stress is significant, and the pressure continues to pass away from the pressure side. Observing the stress of CFRP revealed that the force is more uniform at the same height, and the middle carbon fiber cloth has the most prominent force, which is consistent with the test results. The concrete reinforced by CFRP also breaks in the middle in the axial compression test. By observing the ultimate strain, namely the failure time of the CFRP concrete, it can be found that the law is similar to the peak stress. Only the middle part of the concrete bears more stress while the stress at both ends increases. Compared with the stress at both ends, the intermediate stress of the carbon fiber sheet increases sharply, and the high-stress zone expands until the middle and bottom of the carbon fiber sheet break, failing the entire CFRP-reinforced concrete (Figure 15).

It was found that the simulated values of limit bearing capacity were in excellent conformity with the experimental values. Figure 16 shows the stress–strain relationship simulation results under different reinforcement ratios. It is observed from the results that the peak stress error between the simulated value and the test value is less than 10%. The software analysis values of reclaimed concrete with three

replacement ratios are very close to the stress-strain curves when the reinforcement ratio of carbon fiber fabric is 0%. Compared with the test value, the limit of the simulated value in the descending section should change significantly, as indicated in Figure 16(a). Likewise, the stress-strain curve derived from the simulation analysis reveals that when the reinforcement ratio of carbon fiber cloth is 50%, its slope is larger than the actual test curve, and the peak strain is less than the test value after reaching the proportion limit, as illustrated in Figure 16(b). The software analysis results revealed that the ultimate strain of recycled red brick concrete without reinforcement is more significant than 0.006, close to 0.007, and the ultimate strain of recycled red brick concrete after reinforcement is close to 0.008, which can further predict the internal residual stress under the actual load. Based on the simulated values of carbon fiber-reinforced recycled concrete, it is observed that the stress-strain curves simulated by the software are comparable to the test stress-strain curves of concrete with little error. As a result, the stress-strain curve gained from the software analysis can determine the ductility change of the recycled concrete during the damage phase.

Figure 17 shows the tested and simulated values of peak stresses for specimens with different recycled aggregate replacement rates. The maximum error between the simulated and test values is 5.6%, indicating that the simulation effect is good. Among them, the simulated value of the reclaimed aggregate group without red brick is the best, and the error is the largest when the reclaimed aggregate is 100%. The main reason is that the reclaimed aggregate is dense, loose, and porous, which cannot be simulated entirely, leading to a slightly lower test value than the simulated value. Nevertheless, the simulated values showed a consistent rule with the experimental values. The peak stress showed a decreasing trend with the increase in the replacement rate of red brick aggregate. Compared with the concrete without red brick aggregate, the strength of the specimens with 50 and 100% mixture decreased by 12.5 and 25%, respectively. The increase in the reinforcement ratio can effectively increase the peak stress. Compared with the unreinforced concrete specimens, the strength of semi-reinforced and fully reinforced concrete specimens increases by 29.5 and 43%, respectively, which is consistent with the test results and shows a consistent rule.

# 3.5 Constitutive model analysis

The equation of the stress-strain curve of concrete in an axial compression state is the most basic constitutive

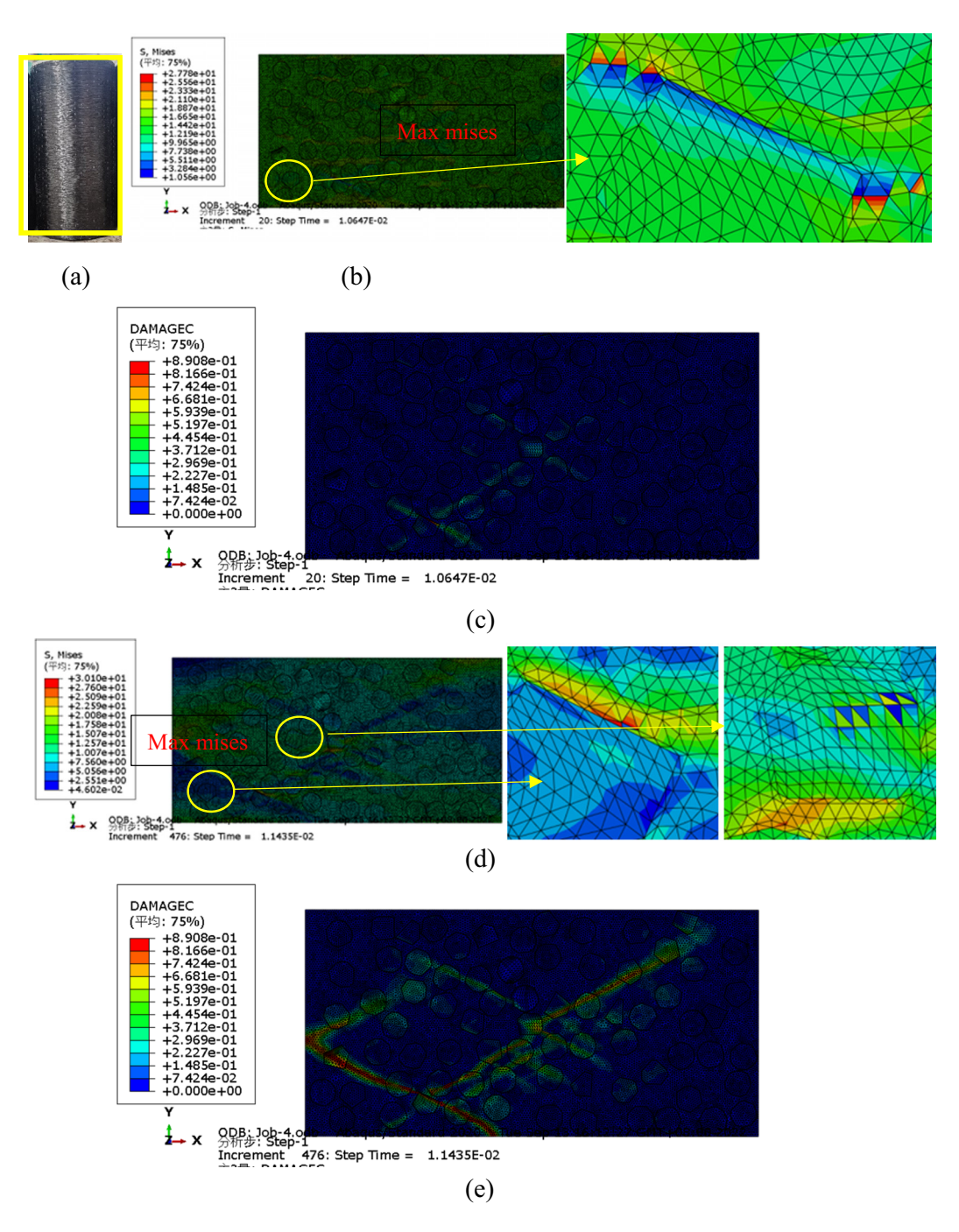


**Figure 14:** Analysis of random aggregate model results: (a) the whole specimen and selected section (b) peak stress; (c) concrete compression damage under peak stress; (d) stress at ultimate strain; and (e) concrete compression damage under ultimate strain;.

relationship to determine the performance of concrete. To accurately express the stress–strain constitutive relation of concrete, the typical model of Guozhenhai was adopted to treat the non-dimensional stress–strain curve of recycled red brick concrete reinforced with carbon fiber cloth under axial compression. In the study,  $\varepsilon/\varepsilon 0$  ( $\varepsilon 0$  is peak strain) is denoted as x, and  $\sigma/fc$  (ratio of stress to peak stress) is denoted as y. The constitutive equation method

proposed by Guo [30] was selected in this study. It provides theoretical support for this study. As mentioned in the study, considering the poor homogeneity of concrete, the curve dispersion of the same group of specimens is large, so it is of no practical significance to select too many curves. Therefore, in this study, the average values of a and b of four specimens in each group were selected as the parameters of the ascending and descending sections

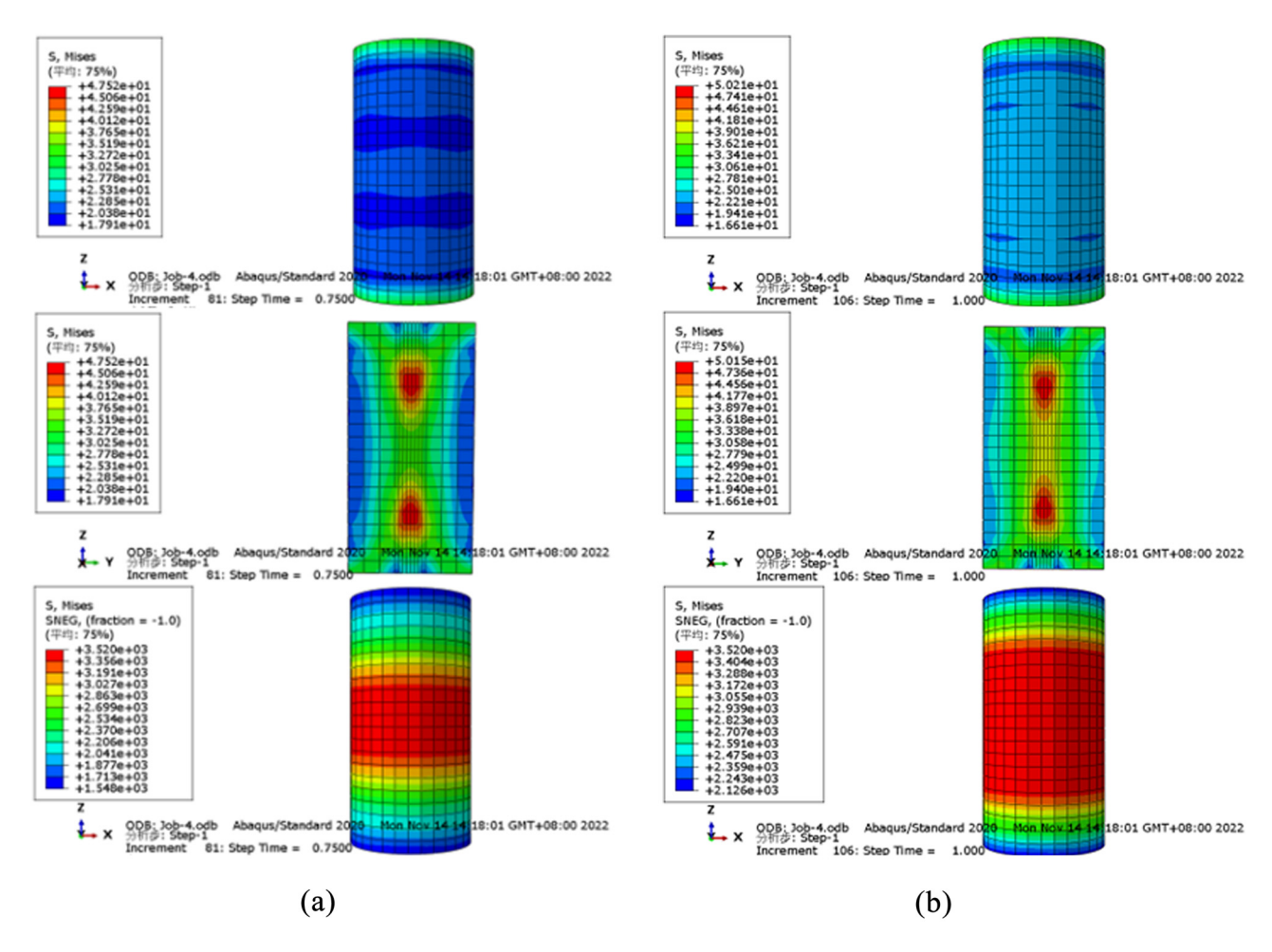


Figure 15: Analysis of concrete and CFRP model results: (a) analysis of the peak stress moment and (b) analysis of the ultimate strain time.

of the group. In this method, a and b are ascending and descending parameters of each stress–strain curve. The curve varies according to material properties controlled by two parameters. Therefore, by varying these two parameters, the stress–strain curves of different specimens can be predicted more accurately. Depending on the parameters of the rising and falling sections (a and b), different aggregate replacement rates r and reinforcement rates  $\theta$  are suggested. The constitutive equation of concrete is as follows:

$$y = ax + (3 - 2a)x^2 + (a - 2)x^3(0 \le x \le 1),$$
 (1)

$$y = \frac{x}{b(x-1)^2 + x} (1 \le x). \tag{2}$$

The parameters of the aggregate replacement rate r determined a and b of the ascending and descending sections  $(0 \le r \le 1)$  and the carbon fiber reinforcement ratio  $\theta$   $(0 \le \theta \le 1)$ . These two parameters control the shape of stress—strain curves at different sections. It turns out that parameters a and b correlate with the regenerated aggregate replacement

rate r and reinforcement ratio  $\theta$  in the form of a nonlinear surface through a nonlinear fitting. The specific rules are shown in Figure 18(a) and (b). Using cubic function fitting to analyze the influence of aggregate replacement rate r and carbon fiber reinforcement ratio  $\theta$  on the parameters a and b in the constitutive equation under the combined influence, a corrected constitutive model for carbon fiber reinforced recycled red brick aggregate concrete was acquired. Among them, red brick's aggregate replacement rate is r, carbon fiber cloth's reinforcement ratio is  $\theta$ , and  $R^2$  is close to 1. Therefore, the constitutive model proposed in this article can accurately work out stress—strain analysis data of carbon fiber cloth recycled concrete reinforced red brick under natural stress in a specific dosage range.

$$a = 1.83 + 0.08r - 0.27\theta + 0.04r^{2} - 0.16\theta^{2} \quad (R^{2} = 0.96),$$
(3)

$$b = 3.68 - 0.27r + 3.4\theta + 0.171r^{2} - 0.69\theta^{2} (R^{2} = 0.99).$$
 (4)

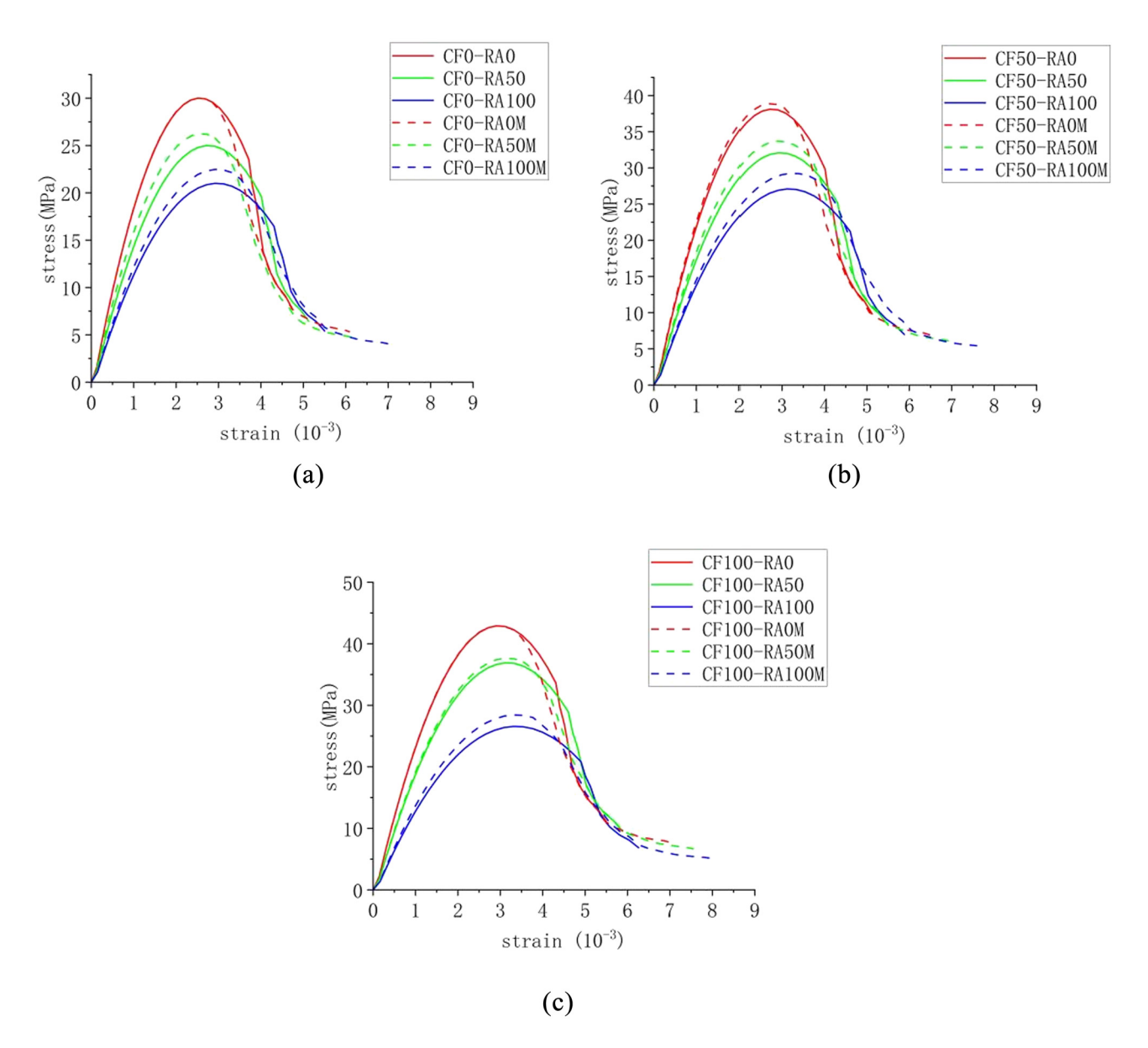


**Figure 16:** Comparison of simulated and tested stress–strain curves: (a) unreinforced recycled concrete; (b) semi-reinforced recycled concrete; and (c) fully reinforced recycled concrete.

Among them, the curve parameters a (1.442  $\le a \le 1.998$ ) in the ascending section and b (3.57  $\le b \le 6.4$ ) in the descending section control the stress–strain curve shapes under the simultaneous action of different red brick content and CFRP reinforcement ratio, respectively. When the reinforcement ratio is 50%, it can be revealed from the fitting formula that the larger the content of recycled aggregate in red brick, the larger the curve parameter a of the ascending section, the gentler the ascending section curve, and the slope decrease with the increase of the content of recycled aggregate. It is mainly because the compactness of the red brick aggregate itself is low, which requires excellent longitudinal strain to give full play to its

maximum bearing capacity. With the increase of recycled aggregate content, curve b of the descending section shows an upward trend, but the corresponding stress–strain curve value of the descending section is tiny. In the same interval, the curve with recycled aggregate content drops more gently. Under the same normalized strain, the higher the red brick content, the lower the concrete stress. Compared with natural aggregate concrete, the decline slope is higher, related to the low strength of red brick aggregate. For the red brick content of 50%, it can be observed that with the increase of CFRP reinforcement ratio after calculation by the fitting formula, the reinforcement ratio has little influence on the curve shape of the

rising section, which is not as apparent as the red brick variable r. It can be observed that the difference between the shape of the rising section of concrete specimens with the exact dosage of 50% is not apparent. Only the curve of the fully reinforced specimens in a short section is slightly gentle before the peak strain. As the reinforcement ratio increases  $\theta$ , the same is true for parameter b in the descending section. If the red brick content remains unchanged, it can be evident that as the reinforcement ratio increases, parameter b in the descending section also increases. However, the overall stress–strain curve becomes lower and more gentle. The overall influence is less severe than the regenerated aggregate replacement rate r. Therefore, it can be concluded that compared with the reinforcement ratio  $\theta$ , the red brick

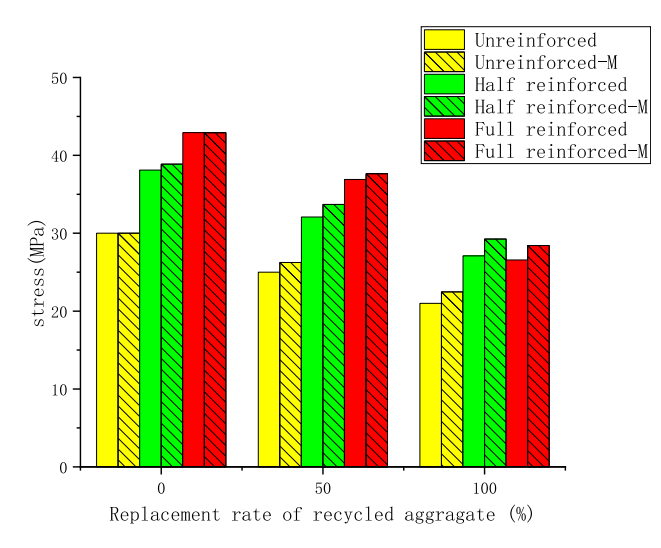
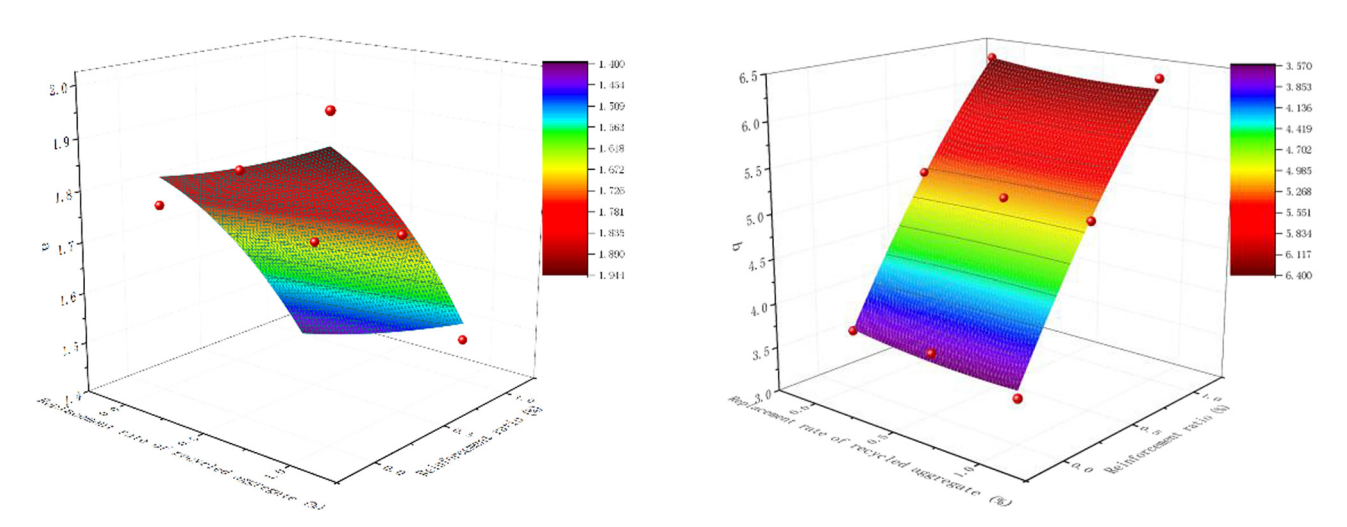


Figure 17: Comparison of simulated and tested peak stresses.

aggregate replacement rate r has a more significant influence on the stress–strain curve. The upward and downward curves are gentler, with the red brick aggregate replacement rate increasing under the same reinforcement ratio.

# 3.6 Effects of reclaimed aggregate and CFRP reinforcement

The effects of aggregate replacement rate and CFRP reinforcement ratio on mechanical properties of red brick recycled concrete were analyzed by selecting mechanical properties indexes and microscopic observation results, respectively. Compressive strength, peak strain, and elastic modulus analyzed in the above tests are selected as mechanical property indexes. It was observed that the influence of red brick's replacement rate on the changing compressive strength trend is negatively correlated, as shown in Figure 6. The strength of reclaimed concrete with a replacement rate of 100% decreases by 29% compared with plain concrete. This phenomenon is mainly due to the poor combination of old mortar on the surface of red brick aggregate with other concrete components. According to this article's test results, the specimen's elastic modulus without adding red brick is the highest, and the elastic modulus of the specimen with a 100% red brick replacement rate is 38% lower than that of ordinary concrete. With the increase of red brick aggregate, the peak strain of axial compression specimens showed an increasing trend. Compared with the specimens without regenerated red brick aggregate, the fractional strain of



**Figure 18:** Nonlinear surface fitting of curve parameters of the constitutive equation: (a) ascending stage parameters and (b) descending stage parameters.

the specimens with 100% red brick replacement rate increased by 16%, mainly because of the excellent ductility of red brick aggregate. From a microscopic point of view, the influence of the addition of red brick aggregate on the strength of concrete is more intuitive. Compared with natural aggregate, it is not easy to be crushed directly during axial compression failure. In contrast, the red brick aggregate is directly crushed through the failure of the reclaimed concrete specimen. This phenomenon is consistent with the first failure of red brick aggregate in the finite element model. It is observed that the size and number of holes in the reclaimed concrete specimens increase with the red brick aggregate replacement rate, and cracks in the ITZ can be obviously observed in the specimens with a 100% red brick aggregate replacement rate. Moreover, due to the differences between red brick aggregate and ordinary concrete elements, more carbonization reaction was generated in the hydration process. The insufficient strength of its elements led to the decline of the strength of reclaimed concrete specimens.

CFRP reinforcement can effectively improve the strength of concrete according to the compressive strength analysis. Compared with unreinforced concrete, the strength of fully reinforced specimens can be increased by 44-48%, and the maximum elastic modulus is 23%. Moreover, the hoop effect of concrete can be further increased to improve the peak strain of the maximum stress under axial compression. Compared with the specimen without reinforcement, the peak strain of the specimen with a 100% reinforcement ratio is increased by 15.5%. It can be revealed from the finite element model that the maximum stress undertaken by CFRP at the peak stress moment is 74% of the maximum stress of the concrete specimen, and the stress undertaken by the carbon fiber cloth in the middle part is greater than that of the concrete in the non-core part. It indicates that the CFRP reinforcement system can bear 43% of the load of the reinforced recycled concrete structure, including itself, while the concrete bears only 57%. When the recycled aggregate content and the reinforcement ratio act simultaneously, they affect the compressive strength, but the reinforcement ratio of CFRP has an influence. For example, the strength of the specimen with 100% red brick composition fully reinforced is greater than that of the plain concrete without reinforcement. However, the replacement rate of recycled aggregate mainly determines the influence on the strain. It can be shown from the stress-strain curve obtained from the test and the proposed constitutive equation that the peak strain gradually increases with the increase of the aggregate substitution rate of red brick because the red brick aggregate can improve the ductility of the specimen. However, the reinforcement ratio has little effect on it.

# 4 Conclusion

To study the mechanical properties and microstructure of CFRP-reinforced red brick recycled concrete, this article conducted an axial compressive strength test, microscopic observation, and element analysis on concrete with different reinforcement ratios and different red brick recycled aggregate content. Furthermore, the damage mechanism of CFRP-reinforced recycled concrete was studied combined with numerical analysis and finite element simulation, and the following conclusions were obtained:

- 1) Compared with ordinary concrete, the compressive strength reduction of 50 and 100% recycled red brick concrete is 14 and 50%, respectively. Therefore, the overall compressive strength of the specimens strengthened by CFRP is higher than those not strengthened. Compared with the specimens not strengthened, the strength of the specimens increased by 27 and 44%, correspondingly, after semi-reinforcement and full-reinforcement treatment.
- The stress-strain curves of the concrete mixed with red bricks are shown to be familiar with the curves of ordinary concrete. With the increase in the replacement rate of recycled aggregates, the peak stress falls, and the peak stress rises. The elastic modulus showed a decreasing trend. Therefore, recycled red brick aggregate and carbon fiber reinforcement can improve its extension and ultimate strain.
- The red brick aggregate has a soft texture and many internal pores, resulting in a generally lower mechanical performance index than natural aggregate. Micro observation shows that the bonding degree between aggregate and mortar in the transition zone differs for concrete specimens with different recycled aggregate replacement rates. Compared with other parts inside the concrete, the bonding of recycled aggregate and mortar in the transition zone of the concrete interface was poor. In addition, during the axial compression test, the red brick aggregate itself is more susceptible to aggregate damage than natural aggregates, thus resulting in a significantly lower strength of specimens containing recycled red brick aggregate than plain concrete specimens at the same reinforcement ratio. The deterioration of the mechanical properties of reclaimed concrete specimens is positively correlated with the replacement rate of reclaimed aggregate.
- The effectiveness of the finite element model is verified by comparing the experimental values, and the effects of red brick aggregate content and carbon fiber sheet reinforcement ratio on the compressive strength of recycled concrete are studied. As a result, the finite

- element simulation results are consistent with the experimental values, and the error is less than 10%. Furthermore, it can be noticed that compared with the content of red brick from the comparison of reinforcement ratios of the different carbon fiber cloth, the reinforcement ratio of carbon fiber cloth has a more significant effect on the strength index of specimens.
- 5) A uniaxial compression model of CFRP-reinforced recycled red brick recycled aggregate concrete was developed based on a nonlinear regression analysis of the stress-strain relationship of carbon fiber-reinforced red brick concrete. Furthermore, a modified model for carbon fiber-reinforced red brick concrete is proposed to precisely determine the stress-strain relationship for CFRP-reinforced recycled red brick concrete.

**Acknowledgments:** The authors would like to acknowledge support from the Fundamental Research Funds for the Central Universities (No. 2572022BJ03) and Science and Technology project of the Heilongjiang Provincial Department of Transportation. Proprietary information such as product names and manufacturers is not included to avoid commercialism.

**Funding information:** The authors would like to acknowledge support from the Fundamental Research Funds for the Central Universities (No. 2572022BJ03) and Science and Technology project of Heilongjiang Provincial Department of Transportation.

**Author contributions:** All authors have accepted responsibility for the entire content of this manuscript and approved its submission.

**Conflict of interest:** The authors state no conflict of interest.

**Data availability statement:** All data generated or analyzed during this study are included in this published article.

# References

- [1] Wu, B., Y. Yu, Z. P. Chen, and X. L. Zhao. Shape effect on compressive mechanical properties of compound concrete containing demolished concrete lumps. *Construction and Building Materials*, Vol. 187, 2018, pp. 50–64.
- [2] Mohammed, T. U., A. Hasnat, S. M. ASCE, M. A. Awal, and S. Z. Bosunia. Recycling of brick aggregate concrete as coarse aggregate. *Journal of Materials in Civil Engineering*, Vol. 27, 2015, pp. 1–9.

- [3] Brito, J. D. and R. Silva. Current status on the use of recycled aggregates in concrete: Where do we go from here. RILEM Technical Letters, Vol. 1, 2016, pp. 1–5.
- [4] Bao, J. W., S. B. Xue, P. Zhang, Z. Z. Dai, and Y. F. Cui. Coupled effects of sustained compressive loading and freeze-thaw cycles on water penetration into concrete. *Structural Concrete*, Vol. 22, 2020, pp. 944–954
- [5] Amorim, P., J. D. Brito, and L. Evangelista. Concrete made with coarse concrete aggregate: influence of curing on durability. ACI Materials Journal, Vol. 109, 2020, pp. 195–204.
- [6] Sunayana, S. and S. V. Barai. Recycled aggregate concrete incorporating fly ash: Comparative study on particle packing and conventional method. *Construction and Building Materials*, Vol. 156, 2017, pp. 376–386.
- [7] Silva, R. V., R. Neves, J. D. Brito, and R. K. Dhir. Carbonation behaviour of recycled aggregate concrete. *Cement and Concrete Composites*, Vol. 62, 2015, pp. 22–32.
- [8] Yang, J., Q. Du, and Y. W. Bao. Concrete with recycled concrete aggregate and crushed clay bricks. *Construction and Building Materials*, Vol. 25, No. 4, 2011, pp. 1935–1945.
- [9] Jie, C., G. Yue, Y. Y. Wang, and W. J. Sun. Basic mechanical properties and stress-strain relationship for recycled concrete including crushed clay bricks. *Journal of Building Structures*, Vol. 4112, 2020, pp. 184–192.
- [10] An, X. Z., W. Niu, Y. Y. Yang, Y. F. Zhang, and Y. Liu. Influence of waste brick coarse aggregate on compressive and shrinkage of recycled concrete. *Journal of Hebei University of Engineering (Natural Science Edition)*, Vol. 34, No. 3, 2017, pp. 56–59 + 73.
- [11] Xiao, J. Z., W. G. Li, Y. H. Fan, and X. Huang. An overview of study on recycled aggregate concrete in China (1996–2011). *Construction and Building Materials*, Vol. 31, 2012, pp. 364–383.
- [12] Ma, Q., Z. L. Hu, Z. Hu, and J. H. Li. Strength characteristics and micro-scale mechanism of high liquid limit clay treated by recycled construction and demolition wastes (CDW) aggregates. Construction and Building Materials, Vol. 332, 2022, pp. 1–13.
- [13] Yang, H., Y. Qin, Y. Liao, and W. Chen. Shear behavior of recycled aggregate concrete after exposure to high temperatures. Construction and Building Materials, Vol. 106, 2016, pp. 374–381.
- [14] Yang, H., D. Liang, Z. Deng, and Y. Qin. Effect of limestone powder in manufactured sand on the hydration products and microstructure of recycled aggregate concrete. *Construction and Building Materials*, Vol. 188, 2018, pp. 1045–1049.
- [15] Zhang, L. W., A. O. Sojobi, and K. M. Liew. Sustainable CFRP-reinforced recycled concrete for cleaner eco-friendly construction. *Journal of Cleaner Production*, Vol. 233, 2019, pp. 56–75.
- [16] Dai, J. G., Y. L. Bai, and J. G. Teng. Behavior and modeling of concrete confined with FRP composites of large deformability. *Journal of Composites for Construction*, Vol. 15, No. 6, 2011, pp. 963–973 + 73.
- [17] Al-Rousan, R. Behavior of circular reinforced concrete columns confined with CFRP. *Journal of Composites for Construction, Procedia Manufacturing*, Vol. 44, No. 6, 2020, pp. 623–630.
- [18] Chen, Z. P., W. S. Xu, and J. Zhou. Mechanical performance of marine concrete filled CFRP-aluminum alloy tube columns under axial compression: Experiment and finite element analysis. *Engineering Structures*, Vol. 272, 2022, pp. 1–16.
- [19] Liu, X., T. Wu, H. X. Chen, and Y. Liu. Compressive stress-strain behavior of CFRP-confined lightweight aggregate concrete reinforced with hybrid fibers. *Composite Structures*, Vol. 244, 2020, pp. 1–16.

- [20] Ramirez, R., H. Maljaee, B. Ghiassi, P. B. Lourenço, and D. V. Oliveira. Bond behavior degradation between FRP and masonry under aggressive environmental conditions. *Mechanics of Advanced Materials and Structures*, Vol. 26, No. 1, 2019, pp. 6–14.
- [21] Yang, S. T., C. Liu, Z. K. Sun, M. Q. Xu, and Y. D. Feng. Effects of resin pre-coating treatment and fibre reinforcement on adhesive bonding between CFRP sheet and concrete. *Composite Structures*, Vol. 292, 2022, pp. 1–22.
- [22] Mostofinejad, D. and B. Arefian. Generic assessment of effective bond length of FRP- concrete joint based on the initiation of debonding: experimental and analytical investigation. *Composite Structures*, Vol. 277, 2022, pp. 1–9.
- [23] Ko, H., S. Matthys, A. Palmieri, and Y. Sato. Development of a simplified bond stress-slip model for bonded FRP–concrete interfaces. Construction and Building Materials, Vol. 68, 2014, pp. 142–157.
- [24] Arefian, B. and D. Mostofinejad. Experimental investigation and modeling of FRP-concrete joint bond strength based on failure depth. *Journal of Composites for Construction*, Vol. 25, No. 6, 2021, pp. 1–13.

- [25] Pebble and crushed stone for construction: GB/T14685-2011, China Architecture & Building Press, Beijing, 2012.
- [26] Techincal code for safety appraisal of engineering structural strengthening materials: GB50728-2011, China Architecture & Building Press, Beijing, 2012.
- [27] Deng, Z., W. Chai, B. Liu, and Y. Hu. Compression behavior of CFRP-confined coral aggregate concrete (CCAC) circular stub columns. *Case Studies in Construction Materials*, Vol. 16, 2022, pp. 1–14.
- [28] Standard for test methods of concrete physical and mechanical properties: GB/T50081-2019, China Architecture & Building Press, Beijing, 2012.
- [29] Yang, H., W. Lan, Y. Qin, and J. Wang. Evaluation of bond performance between deformed bars and recycled aggregate concrete after high temperatures exposure. *Construction and Building Materials*, Vol. 112, 2016, pp. 885–891.
- [30] Guo Z. H., X. Q. Zhang, and D. C. Zhang, Experimental study on full stress-strain curve of concrete. *Journal of Building Structures*, Vol. 1, 1982, pp. 1–12.